Biochemistry

 Volume 33, Number 40 October 11, 1994

Articles

The Retinal Schiff Base–Counterion Complex of Bacteriorhodopsin: Changed Geometry during the Photocycle Is a Cause of Proton Transfer to Aspartate 85†

Leonid S. Brown,‡ Yahaloma Gat,§ Mordechai Sheves,§ Yoichi Yamazaki,‖ Akio Maeda,‖ Richard Needleman,⊥ and Janos K. Lanyi*,‡

Department of Physiology and Biophysics, University of California, Irvine, California 92717, Department of Organic Chemistry, Weizmann Institute of Science, Rehovot, Israel, Department of Biophysics, Faculty of Science, Kyoto University, Kyoto 606-01, Japan, and the Department of Biochemistry, Wayne State University, Detroit, Michigan 48201

Received June 3, 1994; Revised Manuscript Received August 8, 1994®

ABSTRACT: Bacteriorhodopsin contains *all-trans*-retinal linked via a protonated Schiff base to K216. The proton transport in this pump is initiated by *all-trans* to 13-*cis* photoisomerization of the retinal and the ensuing transfer of the Schiff base proton to D85. Changed geometrical relationship of the Schiff base and D85 after the photoisomerization is a possible reason for the proton transfer. We introduced small volume/shape changes with site-specific mutagenesis of residues V49 and A53 that contact the side chain of K216, in order to force the Schiff base into somewhat different positions relative to D85. Earlier [Zimányi, L., Váró, G., Chang, M., Ni, B., Needleman, R., & Lanyi, J. K. (1992) *Biochemistry 31*, 8535–8543] we had described the kinetics of absorbance changes in the microsecond to millisecond time range after photoexcitation with the scheme $L \Leftrightarrow M_1 \Leftrightarrow M_2 + H^+$ (where the first equilibrium is the internal proton transfer and the second is proton release on the extracellular surface). Testing it at various pH values with mutants, where selected rate constants are changed, now confirms the validity of this scheme. The kinetics of the M state thus allowed examination of the transient equilibrium that develops in the $L \Leftrightarrow M_1$ reaction and represents the redistribution of the proton between the Schiff base and D85. From the structure of the protein, the V49A and V49M residue replacements were both predicted to cause decreased alignment of the Schiff base and D85, and indeed we found that they both changed the equilibrium toward the protonated Schiff base. In contrast, the residue replacements A53V and A53G were predicted to move the Schiff base in opposite directions, away from and closer to alignment with D85, respectively. The former indeed changed the equilibrium toward the protonated Schiff base and the latter toward the deprotonated Schiff base. In addition, the hydroxyl stretch band of a bound water in the L state was affected by all mutations that disfavor proton transfer to D85. We conclude that the geometry of the proton donor and acceptor in the Schiff base–D85 pair, mediated by bound water, is a determinant of the proton transfer equilibrium.

The photochemical reaction cycle of the retinal chromophore drives the electrogenic translocation of a proton by bacteriorhodopsin, the proton pump in the cytoplasmic membrane of halobacteria [as reviewed in Mathies et al. (1991), Rothschild (1992), Oesterhelt et al. (1992), Ebrey (1993), and Lanyi (1993)]. The thermal reactions that follow the *all-trans* to 13-*cis* photoisomerization of the retinal are described in a number of reports as a linear sequence of intermediate chromophore states[1] termed J, K, L, M, N, and O (Lozier et al., 1975; Váró & Lanyi, 1990, 1991a,b; Ames & Mathies, 1990; Gerwert et al., 1990; Souvignier & Gerwert, 1992) and substates of several of these. These species are identified by their absorption maxima in the visible, their vibrational spectra, and/or their rise and decay time constants.

† This work was funded partly by grants from the Department of Energy (DEFG03-86ER13525 to J.K.L. and DEFG02-92ER20089 to R.N.), the National Institutes of Health (GM 29498 to J.K.L.), the U.S. Army Research Office (DAAL03-92-G-0406 to R.N.), and the National Science Foundation (MCB-9202209 to R.N.).

* Author to whom correspondence should be addressed.
‡ University of California.
§ Weizmann Institute.
‖ Kyoto University.
⊥ Wayne State University.

® Abstract published in *Advance ACS Abstracts*, September 15, 1994.

0006-2960/94/0433-12001$04.50/0

The first proton transfer in this sequence (the L → M_1 reaction) occurs in the extracellular domain of the protein and consists of the protonation of the anionic D85 by the protonated Schiff base formed by the retinal with the ϵ-amino group of K216. Once D85 is protonated the proton conduction pathway near the Schiff base is reoriented toward the cytoplasmic side (the "reprotonation switch", suggested to be the M_1 → M_2 chromophore reaction). These two crucial steps at the active site initiate the net electrogenic transport of a proton from the cytoplasmic to the extracellular side. They are followed by release of a proton on the extracellular surface, reprotonation of the Schiff base from the protonated D96 in the cytoplasmic region (the M_2 → N reaction), and proton uptake from the cytoplasmic surface.

In the unphotolyzed protein the proton is bound to the Schiff base rather than to D85. Titrations of BR mutants in which residue D85 had been replaced by asparagine or threonine (Brown et al., 1993) suggested that the protonated Schiff base is favored over the protonated D85 by about 30 kJ/mol. In the L state of the photocycle the charged Schiff base–D85 pair ($SBH^+\cdots COO^-$) of the initial state apparently becomes less stable relative to the neutral pair (SB···COOH). According to the kinetics, a transient equilibrium develops between L and M_1, i.e., the states with protonated and deprotonated Schiff bases, respectively, with $K_{eq} = [L]/[M_1] = 4$ (Zimányi et al., 1992b). The free energy gap favoring the protonated Schiff base is thus narrowed to about 3.5 kJ/mol. Although the equilibrium is still not in the direction of proton transfer, this is a small enough $\Delta G°$ to allow the effective deprotonation of the Schiff base under physiological conditions, because at pH ≥ 7 the next step in the photocycle is strongly unidirectional (Váró & Lanyi 1991a,b; Zimányi et al., 1992b).

In principle, there are two kinds of possible causes for the redistribution of the proton between the Schiff base and D85. First, the proton affinity of the Schiff base might be changed by distortion of the electronic configuration along the retinal polyene chain. Calculations indicate that the *trans*-to-*cis* rotation of the C_{13}–C_{14} double bond causes twists in single carbon–carbon bonds, and this will disrupt the π-system of the retinal chain (Schulten & Tavan, 1978; Orlandi & Schulten, 1979; Fahmy et al., 1989). Indeed, the amplitude of the C_{15}–H in-plane vibration at 1303 cm^{-1} is small in the L state, suggesting that the retinal skeleton is twisted in order to remove a steric conflict between the hydrogens on C_{12} and C_{15} (Maeda et al., 1991; Pfefferlé et al., 1991). This would decrease electron density on the Schiff base nitrogen and destabilize the proton (Orlandi & Schulten, 1979; Tavan et al., 1985). Second, because the distal part of the chain and the β-ionone ring of the retinal are firmly fixed by three flanking tryptophan residues (Henderson et al., 1990), isomerization of the C_{13}–C_{14} bond will force the Schiff base to move (Dencher et al., 1992) and assume a different geometrical relationship to D85. Indeed, an increased deuterium shift of the Schiff base C=N frequency (22–24 cm^{-1} in L vs 16 cm^{-1} in BR) indicates that the relationship between the Schiff base and its counterion [and probably water bound by them, cf. de Groot et al. (1990)] becomes altered (Smith et al., 1984; Alshuth & Stockburger, 1986). *Ab initio* calculations of the magnitude and sign of the energy difference between a model charged protonated Schiff base vs carboxylate pair and the corresponding neutral pair indicate that it is considerably dependent on the angle of the hydrogen bond and the polarizability of the environment (Scheiner & Hillenbrand, 1985; Scheiner & Duan, 1991). Results with model compounds and molecular dynamics calculations have suggested that a specific orientation between the Schiff base and the carboxyl group will allow water molecules to adopt a definite structure that forms a bridge between the donor and acceptor groups, stabilizing the ionic interaction (Gat & Sheves, 1993; Humphrey et al., 1994; Sampogna & Honig, 1994). It is probable that changed electron distribution and changed geometry in the L intermediate both contribute to the shift of the Schiff base proton to D85.

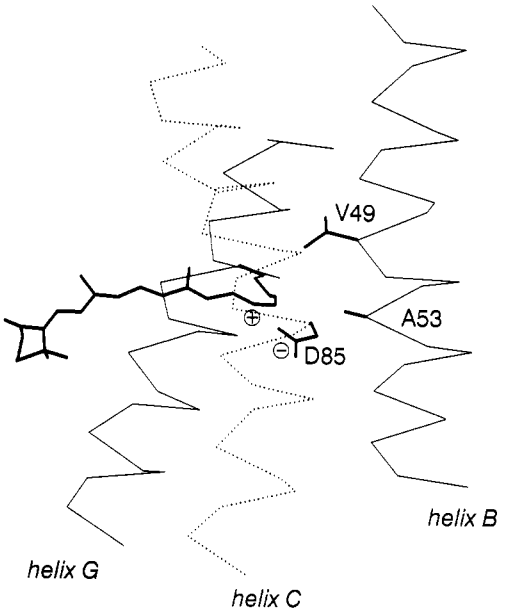

FIGURE 1: Spatial relationship of the Schiff base, D85, V49, and A53 in the structural model of bacteriorhodopsin (Henderson et al., 1990). Helices A, D, E, and F, and other residues are omitted. The *all-trans* retinal is shown in Schiff base linkage (indicated by a positive charge) with K216 on helix G. The closest approaches are as follows: A53, 3.4 Å (to the ϵ-carbon of K216); V49, 3.9 Å (to the ϵ-carbon of K216); D85, 4.2 Å (to the Schiff base nitrogen).

We have explored the second possibility by determining the consequences of small changes in the geometrical relationship of the Schiff base and D85 for the proton transfer equilibrium in the photocycle. The retinal Schiff base is formed with the ϵ-amino group of K216 on helix G. As shown in Figure 1, in the structural model of the protein (Henderson et al., 1990) the residues V49 and A53 on helix B buttress the chain of K216 on helix G and are in position to influence the distance and angle of the Schiff base with respect to D85. In this report we describe the consequences of the V49A, V49M, V49L, A53V, and A53G residue replacements for the proton transfer equilibrium between the Schiff base and D85 during the photocycle.

MATERIALS AND METHODS

Growth of *Halobacterium salinarium* (formerly *H. halobium*) and preparation of purple membranes containing either wild-type or recombinant bacteriorhodopsin were by the standard method (Oesterhelt & Stoeckenius, 1974). The mutants V49A, V49A/D96N, V49A/D115N, V49A/D85N, V49M, V49M/D96N, V49L, A53V, A53V/D96N, A53G, A53G/D96N, D85N, R82Q, R82Q/D96N, Y57F, and Y57F/D96N were constructed and introduced into *H.*

[1] Abbreviations: BR, bacteriorhodopsin; K, L, M, N, and O, photointermediates of the bacteriorhodopsin photocycle, with subscripts for M indicating their access to the extracellular or the cytoplasmic side (M_1 and M_2); site-directed mutants are described with the wild-type and mutated residues separated by the residue number, e.g., V49A; bis-tris-propane, 1,3-bis[[tris(hydroxymethyl)methyl]amino]propane.

salinarium with a shuttle vector containing a novobiocin resistance selection marker to be described elsewhere.

All spectroscopic methods employed have been described in our recent publications (Váró & Lanyi, 1991b; Zimányi & Lanyi, 1993; Cao et al., 1993). Flash excitation was with a frequency-doubled Yag laser (532 nm, 7 ns, Continuum Surelite I). The proton transport activity of bacteriorhodopsin was determined by illuminating cell envelope vesicles in 3 M KCl and measuring the rate of light-dependent pH decrease with a glass electrode. The vesicles were loaded with 3 M KCl (Needleman et al., 1991) and heated at 55 °C for 5 min to inactivate any transport activity due to halorhodopsin or sodium/proton antiport.

The 13-trifluoromethyl retinal analogue was synthesized as before (Sheves et al., 1986). The retinal of the chromophore was replaced in the following way. The membranes were mixed with an equal volume of 2 M neutralized hydroxylamine (freshly made from 4 M NH_2OH and 4 M KOH) and illuminated with yellow light at 22 °C until bleached (Oesterhelt & Schuhmann, 1974; Oesterhelt et al., 1974). They were then repeatedly washed with 100 mM NaCl and 40 mM phosphate, pH 6, to remove the hydroxylamine. Reconstitution was by adding the retinal in 2-propanol to washed bleached membranes (authentic retinal) or by adding the membranes to a test tube after evaporation of methylene chloride and sonicating (analogue), and incubating in either case for 1–14 h.

FTIR spectra were measured with partly hydrated films at pH 7, after 30 s illumination with light at >600 nm, as described before (Maeda et al., 1992, 1994). The L *minus* BR difference spectra were obtained after illumination at 170 K for 2–4 min, and five spectra, each obtained by summing 512 interferograms, were averaged. After each illumination the initial state was to a large extent restored by warming to about 260 K. Light adaptation was at 274 K.

RESULTS

Photocycle of V49A Bacteriorhodopsin. Figure 2 shows difference spectra for V49A at various delays after flash illumination. These spectra differ in four respects from what is observed with the wild-type protein: (1) They become stationary between about 5 and 50 μs where only a small amount of the M state has as yet accumulated. (2) The formation of the M state is slower than in wild type. (3) The absorption amplitude of the M state near 410 nm, once it reaches its maximum at 1–2 ms, is unusually small (about $^1/_5$ of the amplitude in wild type). (4) The time constant for the recovery of the initial BR state at pH 7.4 is about 100 ms, i.e., considerably longer (about 10 times the time constant in wild type).

Deriving the spectra of the K, L, and M states from these measured spectra can be accomplished by a multidimensional grid search method (Zimányi & Lanyi, 1993) in which the calculated spectra are assumed to obey simple criteria such as having only positive amplitudes, a single maximum, etc. The spectra of the intermediates, as well as that of V49A bacteriorhodopsin, are shown in Figure 3A. They are essentially the same as those of the corresponding spectral species in wild type (Váró & Lanyi, 1991b; Zimányi & Lanyi, 1993). The unphotolyzed chromophore had a maximum at 563 nm (Figure 3A). The spectrum of the N state, containing a minor contribution from the O state, could be also reconstructed from the late spectra in the photocycle (not shown). The time-dependent concentrations of the intermediates, calculated by fitting sums of these component difference

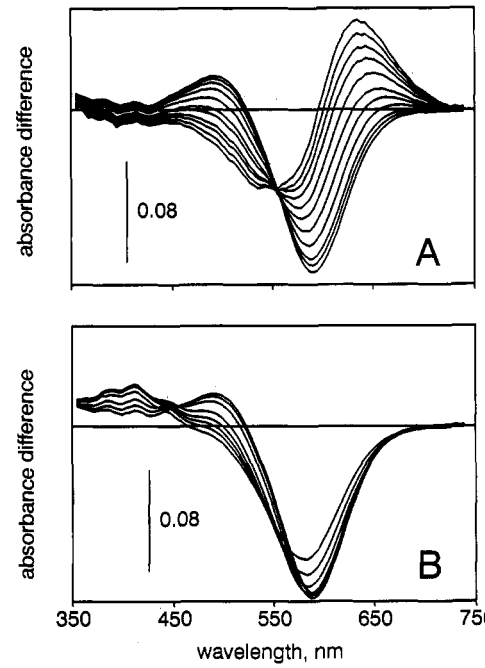

FIGURE 2: Time-resolved difference spectra after photoexcitation of V49A bacteriorhodopsin. Delay time after the flash in panel A (in the direction of decreasing absorbance near 650 nm): 100 ns, 150 ns, 210 ns, 310 ns, 450 ns, 650 ns, 940 ns, 1.4 μs, 2 μs, and 4 μs; in panel B (in the direction of decreasing absorbance near 500 nm): 55 μs, 120 μs, 250 μs, 760 μs, 1.1 ms, 1.6 ms, 2.3 ms, and 3.3 ms. Conditions: 100 mM NaCl, 20 mM bis-tris propane, pH 7.4, and 14 μM bacteriorhodopsin, 25 °C.

spectra to the measured spectra (Figure 2), are shown as points in Figure 3B. A linear model fit these points only with two sequential L and two sequential M states. Neither the two L nor the two M states are spectrally distinguishable from one another. This model with the rate constants of optimal fit, given in the legend to Figure 3, is shown in Figure 3B as lines; the predicted concentration of L_1 is included as a dashed line. For comparison, the kinetics of the M state in the wild-type photocycle under the same conditions is included in Figure 3B as a dotted line.

The photocycle of V49A thus includes an unusually long-lived L [that consists of two substates not readily apparent in the wild type, although L substates have been suggested before, e.g., Zimányi and Lanyi (1993) and Gergely et al. (1993)], and an unusually small amount of M. Under the conditions employed the M intermediate accumulated in V49A to a maximal fractional concentration of about 0.15 (relative to the photocycling fraction), as compared to about 0.85 in wild type. According to the rate constants calculated for the sequential model (Figure 3B, legend), the amount of M in V49A is low because the equilibrium ratio $[L]/[M_1]$, i.e., $K_{eq} = k_{M1L}/k_{LM1}$, is about 22 as compared to 4 in wild type. This would mean that the relative proton affinities of the Schiff base and D85 are changed by the mutation so as to disfavor the proton transfer at this time in the photocycle, the gap between the pK_a's in the proton transfer being increased from 0.6 to 1.3. The two M substates have the same kinetic rationale here as in wild type: a nearly unidirectional reaction between M_1 and M_2 is needed to account for the fact that the decay of L precedes the decay of M in spite of an $[L]/[M]$ equilibrium strongly in favor of L. Because the concentration of M_1 is small, the observed rate of the $M_1 \rightarrow M_2$ reaction will be slow in spite of its not greatly changed rate constant and approach the rate of the decay of M_2, thereby kinetically limiting the amplitude of M. In this model, therefore, it is the greatly

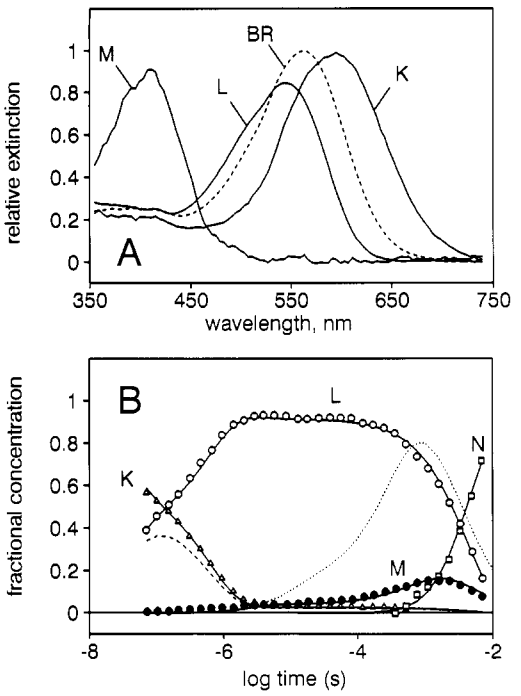

FIGURE 3: Derived spectra of the K, L, and M intermediates of the V49A photocycle (A), and their kinetics (B). In panel A the calculated spectra are shown, together with that of the unphotolyzed chromophore. In panel B the points are the calculated concentrations of K (△), L (○), M (●), and N (□), and the lines are the best fits of the model in the text. The dashed line represents the concentration of the initial L state (cf. text). The kinetic model used was $K \Leftrightarrow L_1 \Leftrightarrow L_2 \Leftrightarrow M_1 \Leftrightarrow M_2 \Leftrightarrow N$. Rate constants ($s^{-1}$): $k_{KL1} = 1.25 \times 10^7$; $k_{L1K} = 1.25 \times 10^7$; $k_{L1L2} = 3.13 \times 10^6$; $k_{L2L1} = 1 \times 10^5$; $k_{L2M1} = 2 \times 10^4$; $k_{M1L2} = 5 \times 10^5$; $k_{M1M2} = 6.25 \times 10^3$; $k_{M2M1} = 10$; $k_{M2N} = 1.27 \times 10^3$; $k_{NM2} = 77$. The dotted line is calculated M kinetics for wild type under these conditions (Váró & Lanyi, 1991a).

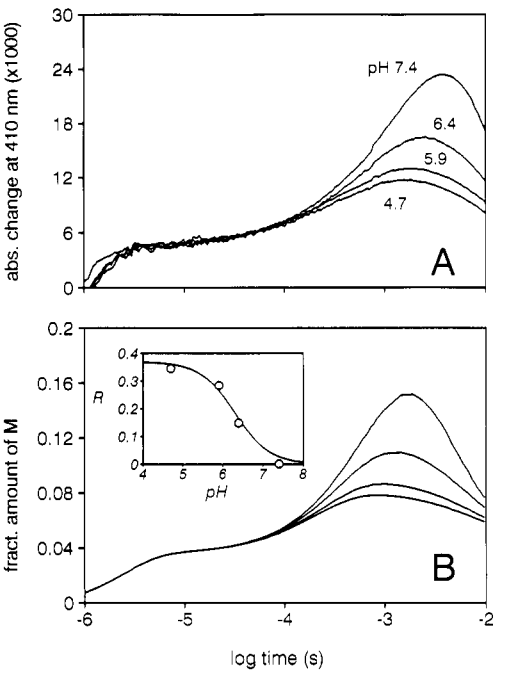

FIGURE 4: Determined (A) and modeled (B) kinetics for the M intermediate in the photocycle of V49A. Panel A shows absorbance changes at 410 nm after photoexcitation at pH 4.7, 5.9, 6.4, and 7.4. Conditions: as in Figure 2, but with 20 mM phosphate as buffer. Panel B shows the predictions of the model, using the rate constants in the legend to Figure 3B, and pH-dependent k_{M2M1} values appropriate for modeling the data. The latter were thus the only variables and are shown in the inset as $R = k_{M2M1}/(k_{M2M1} + k_{M1M2})$ as a function of pH. The four curves in panel B were simulated for the same pH values as in panel A.

diminished accumulation of M_1 that explains why M_2 (and therefore the total amount of M) accumulates to a smaller extent in V49A than in wild type.

Our suggestion that in the V49A mutant the $[L]/[M_1]$ equilibrium is perturbed and reflects thereby a change in the pK_a difference between D85 and the Schiff base depends on whether this kinetic model is correct. There are other possible models. Alternative explanations for the lowered amount of M would be parallel or branched photocycles either containing M or not, originating perhaps from heterogeneity of the unphotolyzed protein. These kinds of schemes have been proposed by several investigators (Diller & Stockburger, 1988; Dancsházy et al., 1988; Bitting et al., 1990; Eisfeld et al., 1993; Hendler et al., 1994) to account for the biphasic M rise and decay kinetics and other complexities in the wild-type photocycle. In the following we describe experiments intended to test the single cycle model and rule out other alternatives.

We had reported earlier that the $M_2 \rightarrow M_1$ back-reaction, not detectable at pH 7, became noticeable at lowered pH, apparently a result of the reversal of the proton release on the extracellular side when the pH is lower than the pK_a of the proton release group (Zimányi et al., 1992b). Because in the kinetic scheme for V49A in Figure 3B $[L]/[M_1]$ is 22 instead of 4 as in wild type, the appearance of such a pH dependent $M_2 \rightarrow M_1$ back-reaction would have a more profound consequence for the total amount of M that accumulates than in wild type. The model was tested therefore by determining the time course of absorption changes at 410 nm at various pH values and comparing the results with its predictions for the kinetics of M. Figure 4 shows measured 410-nm traces at pH between 4.7 and 7.4 and simulated kinetics from the scheme $L \Leftrightarrow M_1 \Leftrightarrow M_2 \rightarrow N$, where the rate constants at pH 7.4 are those determined in Figure 3B, and the only rate constant that varies with pH is that of the $M_2 \rightarrow M_1$ back-reaction (cf. inset in Figure 4B, where the back-reaction rate constant for the M substates divided by the sum of the forward and back-reaction rate constants is shown vs the pH). The model can be made to fit the data for the rise of M reasonably well in this way (no attempt was made to fit the decay of M exactly), and the $M_1 \Leftrightarrow M_2$ rate constants so chosen describe what is expected for the protonation of the extracellular proton release group XH (Zimányi et al., 1992b). As the inset to Figure 4B shows, the apparent pK_a obtained for the proton release is 6.3. In D96N, where such an analysis was first made (Zimányi et al., 1992b) this pK_a was 5.9.

Photocycles of V49A/D96N and V49A/D115N Bacteriorhodopsins. As stated above, according to the proposed model in Figures 3 and 4 based on a single photocycle with a strongly shifted $[L]/[M_1]$ equilibrium for V49A, the accumulation of the total amount of M is small because the rise of M_2 is not much more rapid than its decay. If this is so, slowing the decay of M_2 would raise the concentration of M up to a wild-type-like level, while increasing the rate of the $M_2 \rightarrow M_1$ back-reaction would shift the equilibrium toward L and thereby decrease the concentration of M even further. Schemes in which M arises in a photocycle, or photocycle branch, separate from another cycle or branch not containing M, would not predict such specific changes. We have therefore described the phenotypes of the following two double mutants in which the additional residue replacements should produce the expected effects: (1) D96N, in which the reprotonation of the Schiff base, i.e., M decay, is significantly slowed down (Holz et al., 1989; Butt et al., 1989; Otto et al., 1989; Miller & Oesterhelt, 1990; Cao et al., 1991; Thorgeirsson et al., 1991)

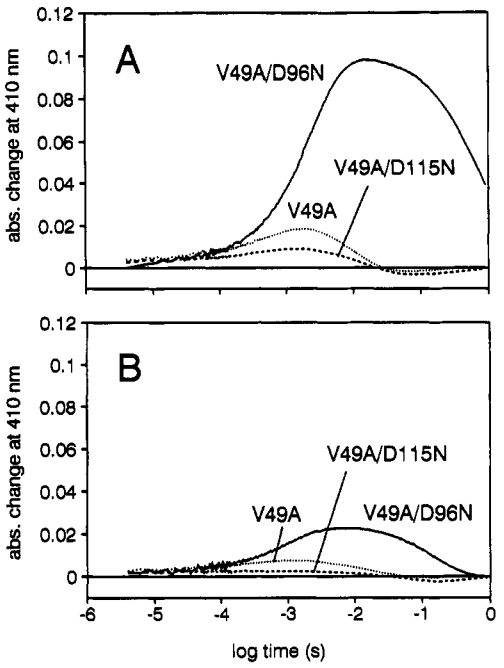

FIGURE 5: M kinetics, as determined from absorbance change at 410 nm after photoexcitation, in V49A, V49A/D96N, and V49A/D115N. Conditions were as in Figure 4. The pH was 7.0 in panel A and 4.0 in panel B.

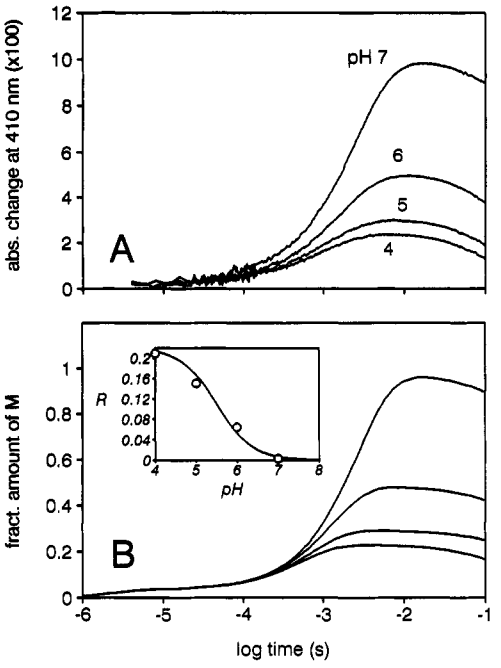

FIGURE 6: Measured (A), and modeled (B), kinetics for the M intermediate in the photocycle of V49A/D96N. Panel A shows absorbance changes at 410 nm after photoexcitation at pH 4, 5, 6, and 7. Conditions were as in Figure 4. Panel B shows the predictions of the model, using the rate constants similar to those in the legend to Figure 3B, but k_{L2M1} was increased to 3.33×10^4 s^{-1} because this is expected for D96N mutants (Zimányi & Lanyi, 1993), and pH-dependent k_{M2M1} values were chosen as appropriate for modeling the data. As in Figure 4, the latter are shown in the inset as $R = k_{M2M1}/(k_{M2M1} + k_{M1M2})$ as a function of pH. The M decay was modeled with the following unidirectional M_2 to N rate constants (s^{-1}): pH 4, 16.7; pH 5, 6.25; pH 6, 3.07; pH 7, 0.93.

and (2) D115N, in which, as described earlier (Zimányi et al., 1992b), for probably structural reasons the rate constant of the $M_2 \rightarrow M_1$ back-reaction is 3 times greater than in wild type. The suggested model for the M kinetics thus predicts that the M amplitude will noticeably increase in V49A/D96N but decrease further in V49A/D115N. Figure 5 compares the absorbance changes at 410 nm after photoexcitation for V49A, V49A/D96N, and V49A/D115N. The pH was 7 for the traces in Figure 5A, and 4 for those in Figure 5B. It is evident that D96N as a second mutation *increases* the amount of M, at the higher pH by a factor of about 6. The amplitude of the transient accumulation of M at its maximum represents in fact nearly 100% of the photocycling fraction of this double mutant, i.e., similar to that in D96N as expected from the model. The near absence of L at this time in the photocycle rules out branched schemes of the type that have M_2 in a *cul-de-sac* from M_1. Figure 5 also shows that D115N as a second mutation strongly *decreases* the amount of M. As expected, at the lower pH the M amplitudes in all mutants are strongly depressed (cf. Figure 4). Remarkably, V49A/D115N under these conditions produces virtually no M (not more than 2–3% of the amplitude in the wild-type photocycle). Further spectroscopic study of the V49A/D115N protein was made very difficult by the fact that in this mutant the decay of the N intermediate is in the second range. In the following, we describe more closely only the V49A/D96N double mutant.

Does the slower M decay explain the expected, and indeed observed, increase in the amount of M in V49A/D96N? Figure 6A shows absorbance traces at 410 nm for V49A/D96N at different pH values. Figure 6B contains simulations of the data with the single cycle model, where nearly the same rate constants were used as for the single mutant in Figure 4B, except for estimations of the strongly decreased and linearly pH dependent (Holz et al., 1989; Miller & Oesterhelt, 1990; Cao et al., 1991) rate constants for the M decay. The good agreement between the observed and simulated M amplitudes indicates that the wild-type-like single-cycle model with shifted $[L]/[M_1]$ equilibrium in Figures 4B and 6B is consistent with the data. As in the case of the single V49A mutant, the pH dependency of the M amplitude is explained by the model as follows. The accumulation of M decreases with decreasing pH because of the increased $M_2 \rightarrow M_1$ back-reaction (i.e., proton uptake linearly dependent on $[H^+]$) that results in shift of the $M_2 \leftrightarrow M_1 \leftrightarrow L$ equilibrium toward L, and therefore the persistence of L in higher concentrations at the lower pH values. The decrease in the amount of M at low pH is more pronounced in these mutants than in the wild type because the $[L]/[M_1]$ equilibrium favors L much more than in the wild type, and since at this time in the photocycle the sum of [L] + [M] is constant, a large increase in [L] will cause a large decrease in [M].

If the increased amplitude of M in the photocycle of V49A/D96N is a simple kinetic consequence of the prolonged lifetime of this state relative to that in V49A, the phenotype of the V49A single mutant should be restored in the double mutant upon addition of azide which decreases the lifetime of M by causing the shuttling of protons to the Schiff base (Tittor et al., 1989). Adding 22 mM azide in experiments with V49A/D96N, as in Figure 5A, indeed strongly decreased the time constant of the decay of M, and its amplitude was accordingly lowered (not shown).

The 13-Trifluoromethyl Retinal Analogue of V49A. The results thus suggest that the V49A residue replacement had caused the ΔpK_a between the Schiff base and D85 in the L state to increase from 0.6 to 1.3. If this is so, replacing the retinal with its 13-trifluoromethyl analogue should restore M accumulation and apparent M rise rate in the mutant to wild-type-like levels, because withdrawal of electrons from the Schiff base nitrogen by the trifluoromethyl group will lower the pK_a of the Schiff base independent of the pK_a of D85 (Sheves et al., 1986). Other models, such as multiple or branched

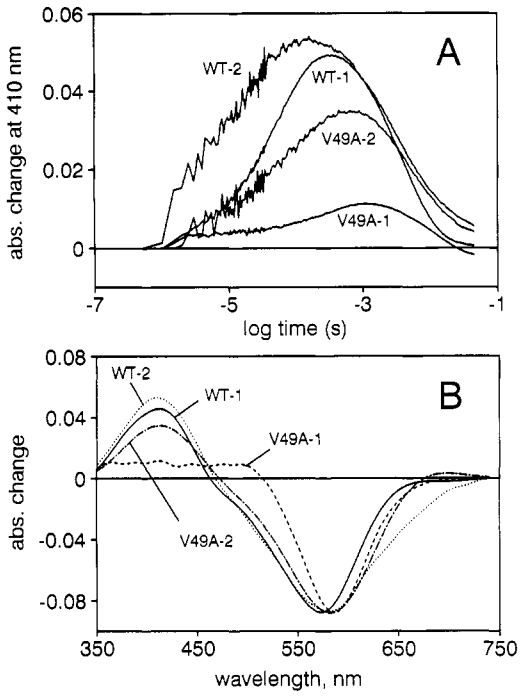

FIGURE 7: Kinetics for the formation of M in V49A and wild-type bacteriorhodopsin, reconstituted with *all-trans*-13-trifluoromethyl retinal and authentic *all-trans*-retinal. WT-1 is wild type containing authentic retinal, WT-2 is wild type containing 13-trifluoromethylretinal, V49A-1 is V49A containing authentic retinal, and V49A-2 is V49A containing 13-trifluoromethylretinal. (A) Absorbance change at 410 nm after photoexcitation. (B) Difference spectra at the time of maximal change at 410 nm after photoexcitation. The time delays were as follows: WT-1, 360 μs; WT-2, 170 μs; V49A-1, 1.1 ms; V49–2, 520 μs. Amplitudes in both panels A and B were normalized to the same depletion. Conditions: 100 mM NaCl, 40 mM phosphate, pH 5.9.

photocycles with unidirectional reactions in which a major pathway lacking M exists parallel with a minor one that contains M, would have no reason to predict such a consequence for the retinal substitution.

Wild-type and V49A bacteriorhodopsins were bleached by illumination in 1 M hydroxylamine, and each was reconstituted with either authentic retinal or the 13-trifluoromethyl retinal analogue. Figure 7A shows 410-nm absorption kinetics (formation and decay of M) for the four samples, while in Figure 7B difference spectra are given at the time of maximal absorbance rise at 410 nm. In the wild-type protein a small increase in the M amplitude when the retinal analogue was used is consistent with more effective deprotonation of the Schiff base, as expected from the lowering of its pK_a. The same effect, but to a considerably greater extent, is seen in V49A. Since in Figure 7 all traces are normalized to the depletion amplitude, for a fair comparison the absorbance increase at 410 nm for the V49A sample with authentic retinal should be divided by approximately 2 to account for the smaller depletion amplitude when little or no M is formed in the photocycle. We estimate that in V49A replacement of the retinal with 13-trifluoromethyl retinal increased the amount of M in the photocycle by a factor of 4–5. Analysis of the rise kinetics as $L \Leftrightarrow M_1 \rightarrow M_2$ gave the result that in wild-type the retinal analogue decreased the $[L]/[M_1]$ ratio from 4 to about 2.5, while in V49A this decrease was from about 20 to about 5. Thus, the results with the retinal analogue are consistent with the model of a wild-type-like photocycle for V49A, one in which the pK_a difference is shifted in favor of the protonated Schiff base.

Proton Transport by V49A and V49A/D115N Bacteriorhodopsins. Cell envelope vesicles were prepared from halobacteria containing either wild-type, V49A, or V49A/D115N bacteriorhodopsin and assayed for light-driven transport activity. The results (not shown) indicate that within measuring error both V49A and V49A/D115N are functionally equivalent to wild type. The decreased amount of M that accumulates in the photocycle of the mutants, particularly in V49A/D115N and at lower pH (Figure 5B, and experiments like in this figure but with the envelope vesicles under the conditions of the transport, not shown), does not result in less transport activity. Remarkably, transport was normal in V49A/D115N at pH 4 where little or no M accumulates. The requirement for the M state, i.e., deprotonation of the Schiff base, in the photocycle for proton translocation had been convincingly demonstrated (Longstaff & Rando, 1987). The necessity of Schiff base deprotonation on the one hand, and the observation of lack of Schiff base deprotonation in a fully transport-active mutant on the other, can be reconciled only by a single photoreaction sequence in which the M state is produced but for kinetic reasons does not accumulate. This constitutes further support of the single cycle model. Wild-type-like transport activity was reported for V49A produced with the *Escherichia coli* expression system also, after its reconstitution into proteoliposomes (Greenhalgh et al., 1993).

pK_a of the Schiff Base in the Unphotolyzed Wild-Type Protein, V49A, D85N, and D85N/V49A. The above results strongly argue that in the L photointermediate of V49A the pK_a difference between the Schiff base and D85 is changed to favor the protonated state of the Schiff base. Does the V49A residue replacement affect the pK_a of the Schiff base in the unphotolyzed state, where the proton transfer is to the protein surface rather than to D85? Further, is the influence of residue 49 in this case on the Schiff base itself, or on the interaction of the Schiff base with D85, as implied by our arguments?

Since the pK_a of the Schiff base in unphotolyzed bacteriorhodopsin is above 13 (Druckmann et al., 1982), the effect of the V49A substitution was studied after replacing the retinal with the 13-trifluoromethyl analogue. In proteins that contain this analogue the pK_a of the Schiff base is in the physiological pH range (Sheves et al., 1986). Figure 8A shows spectroscopic titration of unphotolyzed wild-type and V49A proteins containing 13-trifluoromethyl retinal. As in the photocycle, the apparent pK_a of the Schiff base is raised in the unphotolyzed V49A also, although in this case by only about 0.3 pH units rather than by 0.7 units.

Figure 8B shows the pK_a of the Schiff base in the unphotolyzed V49A/D85N and D85N proteins, as determined by spectroscopic titration. In the absence of the negative charge of D85, the pK_a is considerably lowered (Subramaniam et al., 1990, 1992; Otto et al., 1990; Thorgeirsson et al., 1991; Turner et al., 1993; Brown et al., 1993). Importantly, we find that without a negative charge at position 85, the pK_a is unchanged by the second V49A residue replacement. We conclude that the V49A mutation raises the pK_a of the Schiff base by changing the interaction of the Schiff base and D85, rather than by a direct effect on the Schiff base itself.

The L $\Leftrightarrow$ M_1 Equilibrium in V49L, V49M, A53V, and A53G Bacteriorhodopsins. From the results with V49A we had expected that replacement of V49 with a larger residue and of A53 with a smaller or larger residue would also shift the protonation equilibrium between Schiff base and D85 and in various directions as predicted from the structure of the protein. In the following, results are discussed for V49L,

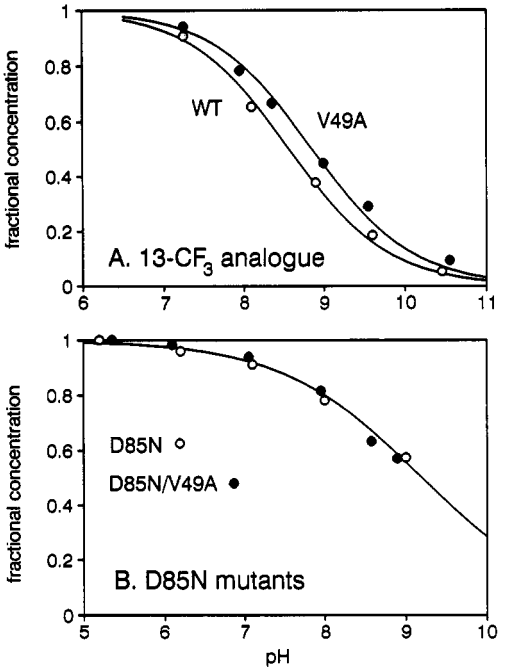

FIGURE 8: Spectroscopic titration of the Schiff base in unphotolyzed bacteriorhodopsins. Spectra were measured in 100 mM NaCl and 40 mM bis-tris propane, at various pH. The decrease in the amplitude of the absorption band near 570–620 nm and the increase of the band near 400–420 nm indicated deprotonation of the Schiff base. The fractional concentration of the protonated Schiff base is shown as function of the pH. (A) wild type (○), and V49A (●), with the retinal replaced by its 13-trifluoromethyl analogue. (B) D85N (○), and D85N/V49A (●).

V49M, A53V, and A53G, as examples of such mutations.

The phenotype of V49L was nearly indistinguishable from that of the wild-type protein. The absorption maximum was at 568 nm, as in wild type, and the L ⇔ M_1 equilibrium in the photocycle was essentially unchanged by the extension of residue 49 by a single methylenic group (not shown).

The V49M and A53V residue replacements produced changed phenotypes, however. Their absorption maxima were at 553 and 548 nm, respectively. Figures 9 and 10 show absorption changes at 410 nm (M kinetics) following photoexcitation of V49M and V49M/D96N, as well as A53V and A53V/D96N, at various pH. The traces for both single mutants (Figures 9A and 10A) distinctly resemble those obtained for V49A (Figure 4) in that (1) the amplitudes are low relative to the wild-type control, (2) the amplitudes increase with pH between 4 or 5 and 7, and (3) the amplitude of the first phase of the formation of M is particularly greatly decreased. For A53V, in fact, the first phase of M formation has too low an amplitude to be observable. Also shown in Figures 9A and 10A are traces for M in the wild type at pH 7; the total amplitude of which is nearly pH independent between pH 4 and 7 (not shown). The M kinetics in the two double mutants (Figures 9B and 10B) are changed in the same way as in V49A/D96N (Figure 6): the amplitudes are much higher and at pH 7 reach that of the wild type, but they are still pH dependent. In analogy with the proposed model for V49A, we interpret the results for V49M and A53V as shifts of the L ⇔ M_1 equilibrium toward L, i.e., increased ΔpK_a between the Schiff base and D85.

The absorption maximum of A53G was 566 nm. For this mutant we would expect that the protonation equilibrium in the photocycle will be shifted *toward* M, i.e., toward decreased ΔpK_a between the Schiff base and D85. Thus, a normal amplitude for M and an increased ratio of [M_1] to [L] relative

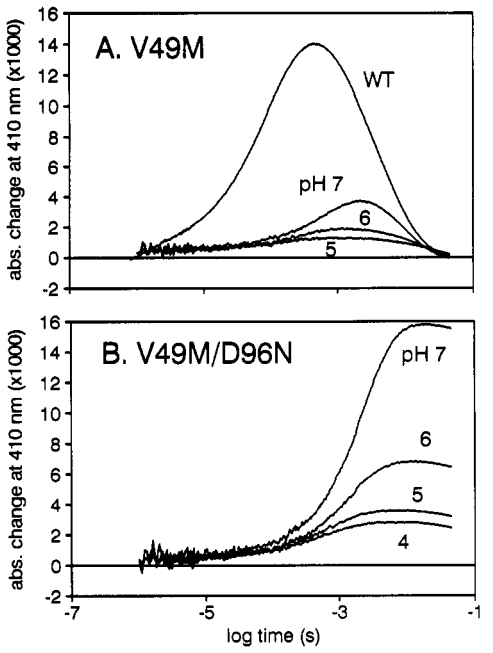

FIGURE 9: M kinetics, as determined from absorbance change at 410 nm after photoexcitation, in V49M and V49M/D96N bacteriorhodopsins at pH 4, 5, 6, and 7 (for V49M the trace at pH 4 was essentially the same as at pH 5). Also included in panel A is a trace for the wild-type protein at pH 7 (labeled as WT). Conditions: 100 mM NaCl and 10 mM phosphate *plus* 10 mM bis-tris propane and 3 μM bacteriorhodopsin (estimated with an extinction coefficient equal to that of wild type).

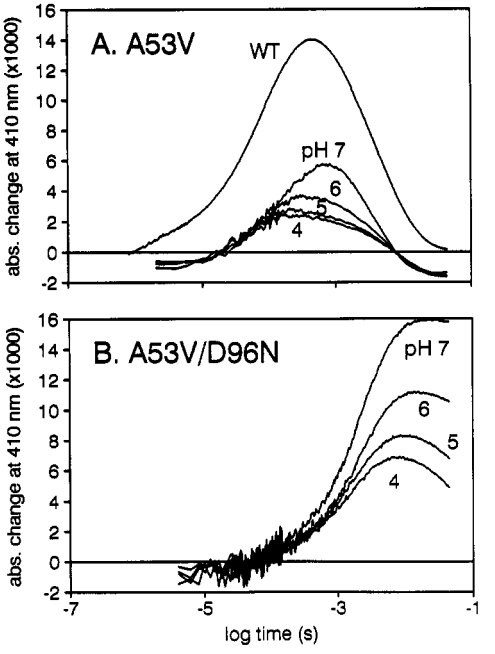

FIGURE 10: M kinetics, as determined from absorbance change at 410 nm after photoexcitation, in A53V and A53V/D96N bacteriorhodopsins at pH 4, 5, 6, and 7. Also included in panel A is a trace for the wild-type protein at pH 7 (labeled as WT). Conditions: 100 mM NaCl and 10 mM phosphate *plus* 10 mM bis-tris propane and 3 μM bacteriorhodopsin (estimated with an extinction coefficient equal to that of wild type).

to the wild type are expected, i.e., a phenotype opposite to those of V49A, V49M, and A53V. The amplitude of M was indeed not lower than in wild type. The formation of the M state in wild type (e.g., under the conditions in Figure 9) was approximated with two kinetic components, with τ_1 = 5 μs, amplitude 13%, and τ_2 = 88 μs, amplitude 87%. In A53G the two M formation components assumed values of τ_1 = 1 μs,

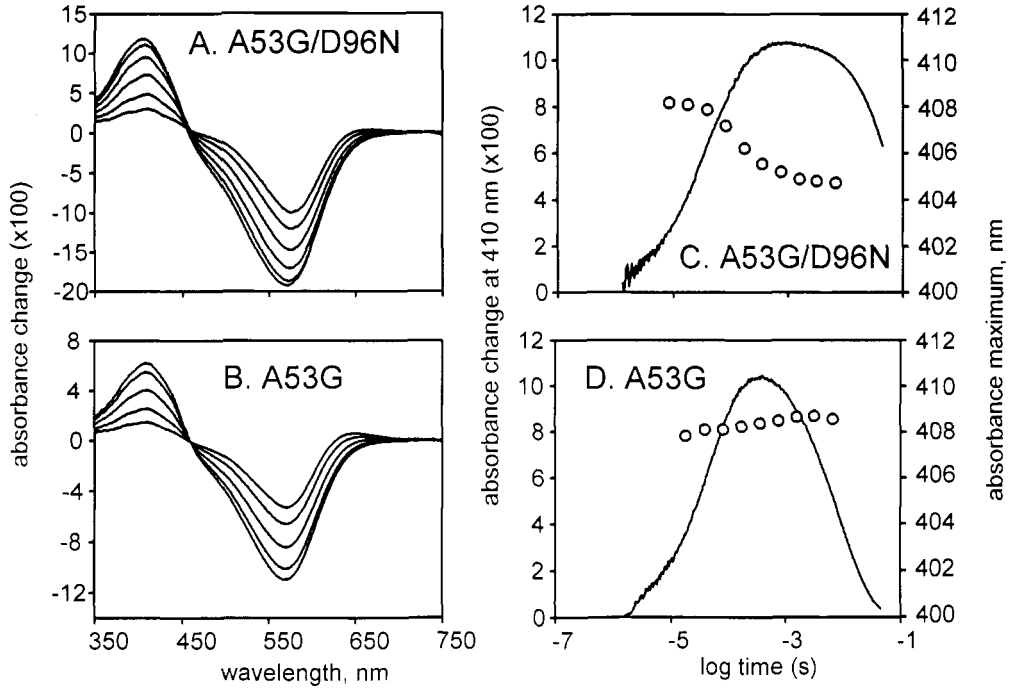

FIGURE 11: M absorption maximum and kinetics, as determined by optical multichannel spectroscopy and from absorbance change at 410 nm after photoexcitation, in A53G/D96N (A and C) and A53G (B and D). (A and B) Difference spectra at 8.4 μs, 17.6 μs, 38.6 μs, 80.2 μs, 169 μs, and 1.6 ms (the last time point is not shown in panel A). (C and D) The traces represent absorbance, the circles the wavelengths of the maxima. The latter were determined by fitting Gaussian curves to the 390–420 nm region of time-resolved difference spectra in panels A and B. For the comparison, the amplitude of the trace in panel D was normalized to that of in panel C. Conditions: 2 M NaCl and 10 mM phosphate *plus* 10 mM bis-tris propane, pH 6.8, and 15 μM bacteriorhodopsin.

amplitude 21%, and τ_2 = 36 μs, amplitude 79%, i.e., the amplitude of the faster component was nearly 2 times that in the wild type, and the equilibration times were much shorter (traces not shown). More rapid formation of M than in wild type was reported earlier for the A53G mutant (Greenhalgh et al., 1993). While this is as expected for an L ⇔ M_1 equilibrium shifted in favor of M_1, demonstration that the greater initial M amplitude indeed represents M_1 is not trivial. We have presented a great deal of evidence here, as well as in earlier reports (Váró & Lanyi, 1991a,b; Zimányi et al., 1992a), in favor of the model L ⇔ M_1 → M_2, where in the wild-type protein at 6 < pH < 10 the first kinetic component for the formation of M (with smaller amplitude) is the equilibration of L and M_1, and the second component (with larger amplitude) is the unidirectional formation of M_2. At pH ≥ 10 the time constant of the M rise is accelerated to about 6 μs. The reaction affected is the L ⇔ M_1 equilibration. This could be demonstrated only in D96N, because through what appears to be loss of interaction of the unprotonated Schiff base with residue 96, the absorption maximum of M_2 (and probably also the later occurring M_N) is blue-shifted, while that of M_1 is unaffected. Thus, during the occurrence of the M_1 → M_2 reaction that is predicted from the decay of the L state the absorption maximum of M shifted from 411 to 404 nm (Zimányi et al., 1992a). We had concluded therefore that the M rise kinetics appeared to be rapid at high pH because M_1 accumulated in increased amounts, and thus the formation of M reflected the formation of M_1 rather than M_2. The approach that utilizes the shift of the maximum of M in D96N mutants to visualize the increased accumulation of M_1 could be applied to the A53G mutant.

Figure 11 contains difference spectra and kinetics for the M intermediate in the photocycles of A53G and A53G/D96N. Panels C and D show M kinetics as measured with absorbance change at 410 nm in the two mutants. Panels A and B show time-resolved difference spectra during the rise phase in the two mutants. Although in other respects these spectra are similar, the maximum near 400 nm shifts distinctly toward lower wavelengths in A53G/D96N, where M_1 and M_2 have different spectra, but not in A53G, where they have the same spectra. The wavelengths of the maxima are superimposed on the kinetics in panels C and D. In D96N under similar conditions there is not a sufficient amount of M at this time during the rise phase to discern the wavelength shift evident at very high pH (Zimányi et al., 1992a; Zimányi & Lanyi, 1993). As before, we interpret the shift of the maximum as the M_1 → M_2 reaction and the results as evidence for the formation of an increased amount of M_1. Thus, the larger amplitude of the first rise component in A53G represents the increased accumulation of M_1, i.e., the protonation equilibrium in this mutant does appear to be shifted in favor of loss of the Schiff base proton. Similar results with R82Q and R82Q/D96N, as well as Y57F and Y57F/D96N (not shown), explain also why in some mutants the formation of the M state is much more rapid than in wild type (Thorgeirsson et al., 1991; Balashov et al., 1993).

FTIR Spectra of the L Intermediates of V49A, V49M, A53V, and A53G in the Hydroxyl Stretch Region. The appearance of a negative band at 3642 cm^{-1} in the L intermediate had shown that in the wild-type photocycle the hydrogen bonding state of one or a few molecules of water is changed (Maeda et al., 1992). Upon $H_2{}^{18}O$ substitution it had become evident that the band shifted to a diffuse range of lower frequencies between 3450 and 3550 cm^{-1}, i.e., weakly interacting water became strongly interacting. The disappearance of this spectral change in the M state and its absence in the L state of the D85N mutant argued that the increased hydrogen bonding of the water depends on both the Schiff base and D85 and implicated it in the proton transfer reaction (Maeda et al., 1994). Figure 12 shows that the 3642-cm^{-1} band has a smaller amplitude, or is perhaps entirely absent, in V49A and A53V. Since the frequency of the band due to

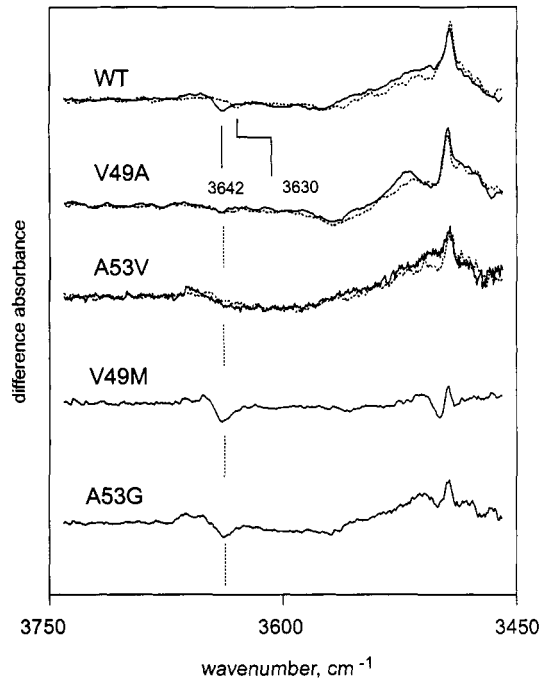

FIGURE 12: Difference (L *minus* BR) FTIR spectra in the hydroxyl stretch region for wild type, V49A, A53V, V49M, and A53G. Solid lines, H_2O; dashed lines, $H_2{}^{18}O$. The amplitudes were scaled to the 1168-cm^{-1} carbon–carbon stretching depletion band.

the hydroxyl stretching of water will be downshifted by about 8 cm^{-1} (cf. the spectrum of the wild type) with $H_2{}^{18}O$, the lack of effect of these substitutions on the increased negative band at 3566 cm^{-1} indicates that this band did not arise by shift of the water band. In V49M the 3642-cm^{-1} depletion band is larger than in wild type, but the increased diffuse absorbance at the lower frequencies is absent. In A53G the changes of the hydroxyl frequencies due to water are about as in wild type. Thus, all mutants where the proton affinities of the Schiff base and D85 are changed so as to favor less proton transfer to D85 show perturbed changes of the water in the L intermediate.

DISCUSSION

How does the absorption of light by the retinal chromophore of bacteriorhodopsin drive proton transport? We suggest that two reactions in the Schiff base–counterion complex account for what is essential in the proton transport: (1) A proton is transferred from the initially high proton affinity Schiff base to the initially low affinity D85 that is part of a complex hydrogen-bonded domain (Harbison et al., 1984; De Groot et al., 1989) with access to the extracellular side. (2) The connection of the Schiff base to the counterion is blocked (Kataoka et al., 1994), allowing reprotonation of the Schiff base from an alternative donor, D96, which is part of a hydrogen-bonded domain with access to the cytoplasmic side (Brown et al., 1994). In this report we are concerned with the reasons for the proton transfer to D85.

The consequence of the photoisomerization of the retinal is that the pK_a difference between the protonated Schiff base and the anionic D85 decreases from about 5.3 to 0.6 (Brown et al., 1993). We have examined the possibility that this change in ΔpK_a is caused, at least in part, by a change in the geometrical relationship of the Schiff base and D85. Introducing volume and shape changes by replacing residues near the hydrocarbon chain of K216, which connects the polypeptide chain to the retinal via the Schiff base, seemed to be a less ambiguous way to influence this relationship than replacing residues near the retinal where they might affect bond rotations in the polyene chain also. Unfortunately, the dispositions of the Schiff base and the residues around it are not known for the L photointermediate, and we have had to rely on structural information for the unphotolyzed protein (Henderson et al., 1990). There are two residues near enough to the hydrocarbon chain of K216 to have possible influence on the spatial position of the Schiff nitrogen. As shown in Figure 1, in the unphotolyzed protein V49 is located on the cytoplasmic side of the lysine chain. In this structural model it comes to within 3.9 Å of the ϵ-carbon of K216. A53, on the other hand, is on the extracellular side of the lysine chain and comes to within 3.4 Å of the ϵ-carbon and 3.6 Å of the γ-carbon. For comparison, the closer of the carboxylate oxygens of D85 (δ-oxygen 2) is 4.2 Å from the Schiff base and 5.2 Å from the β-carbon of A53. Residue A53 is located at the same depth as the Schiff base, while V49 is well to the cytoplasmic side. Thus, we would expect from the structure in Figure 1 that replacing V49 with a smaller or a larger residue would move the Schiff base approximately parallel with the line described by the retinal chain, toward the cytoplasmic or extracellular surface, respectively, but in either case away from its alignment with D85. Replacing A53 with a smaller or larger residue would, on the other hand, move the Schiff base toward D85 or away from alignment with it, respectively, along a line parallel to the membrane surface. These changes should affect both the relationship of the Schiff base to the carboxylate of D85 and the water bound to these groups (Hildebrandt & Stockburger, 1984; Maeda et al., 1992, 1994; Gat & Sheves, 1993; Rath et al., 1993; Deng et al., 1994) and thereby the protonation equilibrium. One would expect that proton transfer from the Schiff base to D85 would be less effective in V49A, V49M, and A53V but more effective in A53G. Accordingly, we describe here the Schiff base–D85 proton transfer equilibrium in the L $\Leftrightarrow$ M_1 reaction in the V49A, V49L, V49M, A53G, and A53V mutants. Since none of these replacements should introduce or remove charges or hydrogen bonds by themselves, the changes observed are interpreted as consequences of the repacking of the protein and the water in this region due to volume and/or shape differences.

Since conclusions about the ΔpK_a must be made from the kinetics of the absorbance changes in the photocycle, we expended a great deal of effort to test and confirm the scheme for the interconversions of L and M from which we derived this parameter, i.e., whether the kinetic parameters do provide the desired equilibrium constant. Using this scheme, we find that small size changes in residues V49 and A53 do change the redistribution of the proton between D85 and the Schiff base in the initial proton transfer reaction of the photocycle. In spite of the approximations used in constructing the structural model (Henderson et al., 1990) and the fact that it refers to the initial state rather than the L photointermediate, it predicts these changes remarkably well. Decreasing the size of residue 49 by two methylene groups increases the ΔpK_a between the Schiff base and D85 from 0.6 to 1.3. Increasing the size of residue 53 by two methyl groups likewise increases the ΔpK_a. Increasing the size of residue 49 by one methylene group has no effect, but the addition of the bulk of a thiomethyl group increases the ΔpK_a. Decreasing the size of residue 53 by a methylene group, on the other hand, notably decreases the ΔpK_a. The results thus indicate that, as expected, the geometrical relationship between the Schiff base and D85 is a critical determinant of the proton transfer process in the L $\rightarrow$ M_1 reaction. The mutations do not affect the pK_a of the Schiff base if D85 is also replaced (Figure 8B). In this sense

the pK_a of the Schiff base is less relevant to the transport than the ΔpK_a between the donor and the acceptor. We suggest that the Schiff base and D85 (and water and protein residues around them that influence their proton affinities) form a hydrogen-bond system, and a reason for the proton transfer is that the photoisomerization of the retinal affects the geometry of this complex.

A high-resolution structure for the immediate vicinity of the Schiff base is not yet available, and at this time we can only speculate about what geometrical changes might occur in the L state. It is important to note, however, that calculations of model systems with a Schiff base and a fixed counterion suggest that minor changes in the distance of charges and in bond angles will cause large changes in the relative energies of a charged donor–acceptor pair and a neutral pair (Scheiner & Hillenbrand, 1985; Scheiner & Duan, 1991). A crude approximation of what might occur is that upon isomerization of the retinal the Schiff base and D85 simply approach one another, and the new relationship they assume shifts the balance of forces toward the proton transfer. On the other hand, the fastest measurable electric signal after photoexcitation ($\tau <$ tens of picoseconds) has the opposite sign from the direction of the net proton translocation [reviewed in Keszthelyi and Ormos (1989)]. If its interpretation as the displacement of the positively charged Schiff base is correct, the Schiff base would move away from D85 rather than toward it. Furthermore, a change of the distance between the Schiff base and D85 in the mutants described would have caused distinct and predictable shifts in the absorption maxima from the wild type. The observed shifts were in fact small and not consistent with any simple distance changes. It is likely that the changed geometry, both in these mutants and what happens in the wild-type protein after the photoisomerization, might involve instead changes in the bond angle between the Schiff base nitrogen and D85 and the way water is bound in this region. This possibility was proposed on the basis of model compound studies (Gat & Sheves, 1993). Arguments for bound water in this region have been made before (Hildebrandt & Stockburger, 1984; Papadopoulos et al., 1990; de Groot et al., 1990; Maeda et al., 1992, 1994; Rath et al., 1993; Deng et al., 1994), and a change in the binding of water by D85 was in fact demonstrated in the L state (Maeda et al., 1992, 1994). We provide direct evidence in this report (Figure 12) that the stronger binding of water in L is altered when the geometry of the Schiff base and D85 is less favorable for proton transfer, but not when it is more favorable.

The results we report strongly suggest that the residues near the Schiff base are packed closely enough to immobilize them. Molecular dynamics simulations support this possibility (Humphrey et al., 1994). The close packing near the Schiff base implies the coupling of the isomerization-induced motions of the retinal to the movement of protein residues in this region, as suggested by dynamic changes in the configuration of the chain of K216 during the photocycle (McMaster & Lewis, 1988; Gat et al., 1992), and by the finding that a covalent bond between residue 216 and a protonated Schiff base is not necessary for the transport function (Schweiger et al., 1994; Friedman et al., 1994).

ACKNOWLEDGMENT

We thank Dr. W. Wimley for making a program to manipulate atomic coordinates available for the computer graphics.

REFERENCES

Alshuth, T., & Stockburger, M. (1986) *Photochem. Photobiol. 43*, 55–66.

Ames, J. B., & Mathies, R. A. (1990) *Biochemistry 29*, 7181–7190.

Balashov, S. P., Govindjee, R., Kono, M., Imasheva, E., Lukashev, E., Ebrey, T. G., Crouch, R. K., Menick, D. R., & Feng, Y. (1993) *Biochemistry 32*, 10331–10343.

Bitting, H. C., Jang, D.-J., & El-Sayed, M. A. (1990) *Photochem. Photobiol. 51*, 593–598.

Brown, L. S., Bonet, L., Needleman, R., & Lanyi, J. K. (1993) *Biophys. J. 65*, 124–130.

Brown, L. S., Yamazaki, Y., Maeda, A., Sun, L., Needleman, R., & Lanyi, J. K. (1994) *J. Mol. Biol. 239*, 401–414.

Butt, H.-J., Fendler, K., Bamberg, E., Tittor, J., & Oesterhelt, D. (1989) *EMBO J. 8*, 1657–1663.

Cao, Y., Váró, G., Chang, M., Ni, B., Needleman, R., & Lanyi, J. K. (1991) *Biochemistry 30*, 10972–10979.

Cao, Y., Brown, L. S., Needleman, R., & Lanyi, J. K. (1993) *Biochemistry 32*, 10239–10248.

Dancsházy, Z., Govindjee, R., & Ebrey, T. G. (1988) *Proc. Natl. Acad. Sci. U.S.A. 85*, 6358–6361.

De Groot, H. J. M., Harbison, G. S., Herzfeld, J., & Griffin, R. G. (1989) *Biochemistry 28*, 3346–3353.

De Groot, H. J. M., Smith, S. O., Courtin, J., Van den Berg, E., Winkel, C., Lugtenburg, J., Griffin, R. G., & Herzfeld, J. (1990) *Biochemistry 29*, 6873–6883.

Dencher, N. A., Heberle, J., Büldt, G., Höltje, H.-D., & Höltje, M. (1992) in *Membrane Proteins: Structures, Interactions and Models* (Pullman, A., Jortner, J., & Pullman, B., Eds) pp 69–84, Kluwer Academic Publishing, Dordrecht, The Netherlands.

Deng, H., Huang, L., Callender, R., & Ebrey, T. (1994) *Biophys. J. 66*, 1129–1136.

Diller, R., & Stockburger, M. (1988) *Biochemistry 27*, 7641–7651.

Druckmann, S., Ottolenghi, M., Pande, A., Pande, J., & Callender, R. H. (1982) *Biochemistry 21*, 4953–4959.

Ebrey, T. G. (1993) in *Thermodynamics of Membranes, Receptors and Channels* (Jackson, M., Ed.) pp 353–387, CRC Press, New York.

Eisfeld, W., Pusch, C., Diller, R., Lohrmann, R., & Stockburger, M. (1993) *Biochemistry 32*, 7196–7215.

Fahmy, K., Siebert, F., Grossjean, M. F., & Tavan, P. (1989) *J. Mol. Struct. 214*, 257–288.

Friedman, N., Druckmann, S., Lanyi, J. K., Needleman, R., Lewis, A., Ottolenghi, M., & Sheves, M. (1994) *Biochemistry 33*, 1971–1976.

Gat, Y., & Sheves, M. (1993) *J. Am. Chem. Soc. 115*, 3772–3773.

Gat, Y., Grossjean, M., Pinevsky, I., Takei, H., Rothman, Z., Sigrist, H., Lewis, A., & Sheves, M. (1992) *Proc. Natl. Acad. Sci. U.S.A. 89*, 2434–2438.

Gergely, C., Ganea, C., Groma, G., & Váró, G. (1993) *Biophys. J. 65*, 2478–2483.

Gerwert, K., Souvignier, G., & Hess, B. (1990) *Proc. Natl. Acad. Sci. U.S.A. 87*, 9774–9778.

Greenhalgh, D. A., Farrens, D. L., Subramaniam, S., & Khorana, H. G. (1993) *J. Biol. Chem. 268*, 20305–20311.

Harbison, G. S., Smith, S. O., Pardoen, J. A., Winkel, C., Lugtenburg, J., Herzfeld, J., Mathies, R. A., & Griffin, R. G. (1984) *Proc. Natl. Acad. Sci. U.S.A. 81*, 1706–1709.

Henderson, R., Baldwin, J. M., Ceska, T. A., Zemlin, F., Beckmann, E., & Downing, K. H. (1990) *J. Mol. Biol. 213*, 899–929.

Hendler, R. W., Dancsházy, Z., Bose, S., Shrager, R. I., & Tokaji, Z. (1994) *Biochemistry 33*, 4606–4610.

Hildebrandt, P., & Stockburger, M. (1984) *Biochemistry 23*, 5539–5548.

Holz, M., Drachev, L. A., Mogi, T., Otto, H., Kaulen, A. D., Heyn, M. P., Skulachev, V. P., & Khorana, H. G. (1989) *Proc. Natl. Acad. Sci. U.S.A. 86*, 2167–2171.
Humphrey, W., Logunov, I., Schulten, K., & Sheves, M. (1994) *Biochemistry 33*, 3668–3678.
Kataoka, M., Kamikubo, H., Tokunaga, F., Brown, L. S., Yamazaki, Y., Maeda, A., Sheves, M., Needleman, R., & Lanyi, J. K. (1994) *J. Mol. Biol.* (in press).
Keszthelyi, L., & Ormos, P. (1989) *J. Membr. Biol. 109*, 193–200.
Lanyi, J. K. (1993) *Biochim. Biophys. Acta 1183*, 241–261.
Longstaff, C., & Rando, R. R. (1987) *Biochemistry 26*, 6107–6113.
Lozier, R. H., Bogomolni, R. A., & Stoeckenius, W. (1975) *Biophys. J. 15*, 955–963.
Maeda, A., Sasaki, J., Pfefferlé, J.-M., Shichida, Y., & Yoshizawa, T. (1991) *Photochem. Photobiol. 54*, 911–921.
Maeda, A., Sasaki, J., Shichida, Y., & Yoshizawa, T. (1992) *Biochemistry 31*, 462–467.
Maeda, A., Sasaki, J., Yamazaki, Y., Needleman, R., & Lanyi, J. K. (1994) *Biochemistry 33*, 1713–1717.
Mathies, R. A., Lin, S. W., Ames, J. B., & Pollard, W. T. (1991) *Annu. Rev. Biophys. Biophys. Chem. 20*, 491–518.
McMaster, E., & Lewis, A. (1988) *Biochem. Biophys. Res. Commun. 156*, 86–91.
Miller, A., & Oesterhelt, D. (1990) *Biochim. Biophys. Acta 1020*, 57–64.
Needleman, R., Chang, M., Ni, B., Váró, G., Fornes, J., White, S. H., & Lanyi, J. K. (1991) *J. Biol. Chem. 266*, 11478–11484.
Oesterhelt, D., & Schuhmann, L. (1974) *FEBS. Lett. 44*, 262–265.
Oesterhelt, D., & Stoeckenius, W. (1974) *Methods Enzymol. 31*, 667–678.
Oesterhelt, D., Schuhmann, L., & Gruber, H. (1974) *FEBS. Lett. 44*, 257–261.
Oesterhelt, D., Tittor, J., & Bamberg, E. (1992) *J. Bioenerg. Biomembr. 24*, 181–191.
Orlandi, G., & Schulten, K. (1979) *Chem. Phys. Lett. 64*, 370–374.
Otto, H., Marti, T., Holz, M., Mogi, T., Lindau, M., Khorana, H. G., & Heyn, M. P. (1989) *Proc. Natl. Acad. Sci. U.S.A. 86*, 9228–9232.
Otto, H., Marti, T., Holz, M., Mogi, T., Stern, L. J., Engel, F., Khorana, H. G., & Heyn, M. P. (1990) *Proc. Natl. Acad. Sci. U.S.A. 87*, 1018–1022.
Papadopoulos, G., Dencher, N. A., Zaccai, G., & Büldt, G. (1990) *J. Mol. Biol. 214*, 15–19.
Pfefferlé, J.-M., Maeda, A., Sasaki, J., & Yoshizawa, T. (1991) *Biochemistry 30*, 6548–6556.
Rath, P., Marti, T., Sonar, S., Khorana, H. G., & Rothschild, K. J. (1993) *J. Biol. Chem. 268*, 17742–17749.
Rothschild, K. J. (1992) *J. Bioenerg. Biomembr. 24*, 147–167.
Sampogna, R. V., & Honig, B. (1994) *Biophys. J. 66*, 1341–1352.
Scheiner, S., & Hillenbrand, E. A. (1985) *Proc. Natl. Acad. Sci. U.S.A. 82*, 2741–2745.
Scheiner, S., & Duan, X. (1991) *Biophys. J. 60*, 874–883.
Schulten, K., & Tavan, P. (1978) *Nature 272*, 85–86.
Schweiger, U., Tittor, J., & Oesterhelt, D. (1994) *Biochemistry 33*, 535–541.
Sheves, M., Albeck, A., Friedman, N., & Ottolenghi, M. (1986) *Proc. Natl. Acad. Sci. U.S.A. 83*, 3262–3266.
Smith, S. O., Myers, A. B., Pardoen, J. A., Winkel, C., Mulder, P. P. J., Lugtenburg, J., & Mathies, R. A. (1984) *Proc. Natl. Acad. Sci. U.S.A. 81*, 2055–2059.
Souvignier, G., & Gerwert, K. (1992) *Biophys. J. 63*, 1393–1405.
Subramaniam, S., Marti, T., & Khorana, H. G. (1990) *Proc. Natl. Acad. Sci. U.S.A. 87*, 1013–1017.
Subramaniam, S., Greenhalgh, D. A., & Khorana, H. G. (1992) *J. Biol. Chem. 267*, 25730–25733.
Tavan, P., Schulten, K., & Oesterhelt, D. (1985) *Biophys. J. 47*, 415–430.
Thorgeirsson, T. E., Milder, S. J., Miercke, L. J. W., Betlach, M. C., Shand, R. F., Stroud, R. M., et al. (1991) *Biochemistry 30*, 9133–9142.
Tittor, J., Soell, C., Oesterhelt, D., Butt, H.-J., & Bamberg, E. (1989) *EMBO J. 8*, 3477–3482.
Turner, G. J., Miercke, L. J. W., Thorgeirsson, T. E., Kliger, D. S., Betlach, M. C., & Stroud, R. M. (1993) *Biochemistry 32*, 1332–1337.
Váró, G., & Lanyi, J. K. (1990) *Biochemistry 29*, 2241–2250.
Váró, G., & Lanyi, J. K. (1991a) *Biochemistry 30*, 5008–5015.
Váró, G., & Lanyi, J. K. (1991b) *Biochemistry 30*, 5016–5022.
Zimányi, L., & Lanyi, J. K. (1993) *Biophys. J. 64*, 240–251.
Zimányi, L., Cao, Y., Chang, M., Ni, B., Needleman, R., & Lanyi, J. K. (1992a) *Photochem. Photobiol. 56*, 1049–1055.
Zimányi, L., Váró, G., Chang, M., Ni, B., Needleman, R., & Lanyi, J. K. (1992b) *Biochemistry 31*, 8535–8543.